



Influence of Boundary Conditions and Internal Fluid Types on Dynamic Characteristics of a Deepwater Riser

Lei Guo

College of Electromechanical Engineering, Changsha University, Changsha, China., leiguo@ccsu.edu.cn

Zong-Ming Zhu

College of Electromechanical Engineering, Changsha University, Changsha, China

Zhong-Jian Pan

College of Electromechanical Engineering, Changsha University, Changsha, China

Zhi-Ming Guo

College of Electromechanical Engineering, Changsha University, Changsha, China

Follow this and additional works at: <https://jmstt.ntou.edu.tw/journal>



Part of the [Fresh Water Studies Commons](#), [Marine Biology Commons](#), [Ocean Engineering Commons](#), [Oceanography Commons](#), and the [Other Oceanography and Atmospheric Sciences and Meteorology Commons](#)

Recommended Citation

Guo, Lei; Zhu, Zong-Ming; Pan, Zhong-Jian; and Guo, Zhi-Ming (2022) "Influence of Boundary Conditions and Internal Fluid Types on Dynamic Characteristics of a Deepwater Riser," *Journal of Marine Science and Technology*: Vol. 30: Iss. 2, Article 3.

DOI: 10.51400/2709-6998.2570

Available at: <https://jmstt.ntou.edu.tw/journal/vol30/iss2/3>

This Research Article is brought to you for free and open access by Journal of Marine Science and Technology. It has been accepted for inclusion in Journal of Marine Science and Technology by an authorized editor of Journal of Marine Science and Technology.

RESEARCH ARTICLE

Influence of Boundary Conditions and Internal Fluid Types on Dynamic Characteristics of a Deepwater Riser

Lei Guo*, Zong-Ming Zhu, Zhong-Jian Pan, Zhi-Ming Guo

College of Electromechanical Engineering, Changsha University, Changsha, China

Abstract

Deepwater Steel Catenary Riser (DSCR) is the key structure of oil and gas production system in the ocean. To design an optimized DSCR system, the dynamic characteristics of the DSCR are analyzed by setting some different boundary conditions and internal fluid types. The main vibration mode of the DSCR is found orthogonal to both mass and stiffness according to the normalization condition of the main mode, and then the regular mode function and the j th order principal stiffness K_{pj} are obtained. Under different initial conditions, the transverse responses of DSCR represented by regular coordinates under arbitrary excitation are obtained. Then, a dynamic model induced by both axial load and transverse load is reconstructed for comparative study, and the axial load is found to have a great effect on the transverse dynamic characteristics. The effects of internal fluid and boundary conditions on the natural frequency of DSCR are also found at last.

Keywords: Riser model, Dynamic characteristics, Boundary effect, Natural frequency

1. Introduction

Oil and gas resources on land can no longer meet human needs because of the rapid development of industry, then it has become a trend to exploit ocean resources vigorously. In the past decade, the growth of global oil and gas production is mainly from offshore oil and gas fields, with nearly 90% deepwater areas [17]. As a key structure of subsea production system, DSCR is widely used to exploit deepwater oil and gas resources [11]. Because of the simple structure, low cost and easy processing, DSCR is widely used in West Africa and the South China Sea.

DSCR is usually suspended directly to a floating platform, and is sensitive to the motion of the floating platform in addition to wind, wave and current. To ensure the safe service of a DSCR, it is necessary to consider the dynamic limit stress and

fatigue [7]. Due to the excitation of current, wave and floating platform motion, significant dynamic stress generates at the suspension end of the DSCR. When the natural frequency of a DSCR is within the range of most excitation frequencies, a large dynamic response, and even resonance will occur.

At present, the dynamic analysis of risers mainly include: time domain analysis, steady-state frequency domain analysis and random vibration analysis [6]. There are two main models used for DSCR in the dynamic response analysis: beam model and catenary model. Beam model is a classical model used to study the dynamic problems of risers, e.g., the dynamic characteristics of DSCR are studied by using a large deflection slender beam model [3]. And in the laying process of J-type riser, the large deformation vibration and buckling of the riser under extreme load are studied by using large deformation beam theory [12,15]. In addition,

Received 23 February 2021; revised 31 May 2021; accepted 26 November 2021.
Available online 17 May 2022.

* Corresponding author. College of Electromechanical Engineering, Changsha University, NO. 98, Hongshan Road, Kaifu District, Changsha, China.
E-mail address: leiguo@ccsu.edu.cn (L. Guo).



catenary model is an effective way to study the overall dynamic characteristics of DSCRs [9].

Due to the large slenderness ratio of the DSCR, the fluid–structure interaction response presents strong nonlinear characteristics. Recent studies show that the vortex induced vibration (VIV) of DSCR becomes more and more complex with the increase depth of service water, and some new features and phenomena appear [4,8,13]. However, there are two problems in the research of fluid–structure interaction of the DSCR: one is that the finite element method encounters the grid distortion caused by moving interface, and it cannot transfer the information of fluid structure interface accurately [14]; the other is that the influence of fluid inside and outside the riser as well as the moving of floating platform are not fully considered in the construction of a dynamic model. The parameters of velocity, density and multiphase flow have a significant influence on the vibration frequency of the riser.

Previous experimental results show that the vibration characteristics of the riser under the combined action of internal and external fluids are significantly different from that under the separate action of internal and external fluids [5]. The flowing fluid in the riser can reduce the stiffness of the structure and produce negative damping, which reduces the natural frequency of the riser [10]. When the velocity of fluid in the riser is significantly larger than that of the external fluid, internal flow factors determine the vibration frequency, vibration intensity and instantaneous amplitude [1]. Then, different internal or external flow velocity, viscosity coefficient and whether the internal and external flow act together have a great difference [2].

In this paper, a new dynamic model of DSCR considering the effect of internal fluid is constructed. By deriving the vibration differential equation and response function of the DSCR, the characteristics of the main vibration mode are investigated. The natural frequency of the DSCR is found to change with boundary conditions and internal fluid state, and the overall effect of the internal fluid on the transverse vibration characteristics of the riser is further studied. The study is helpful for finding an effective measure to avoid the vibration damage and can provide theoretical reference for the safe service and fatigue life prediction of DSCRs.

2. Dynamic model with only transverse loads

2.1. Construction of dynamic model

This paper focuses on the influence of boundary conditions and internal fluid types on the dynamic

characteristics of the DSCR. The influence of sea surface waves can be ignored in case of calm sea surface. Therefore, this part only considers the loads caused by ocean current below the sea surface.

When the DSCR transports natural gas or it is an empty riser, the axial force generated by the dead weight of the riser and the seawater buoyancy is very small. To analyze the transverse dynamic characteristics of the DSCR only under the action of transverse force, the axial force is assumed to be 0. Firstly, a model without considering the axial loads is constructed. The forces on the DSCR are shown in Fig. 1.

Taking the micro element with a length of dz on the riser as the analysis object (see Fig. 2), at any instant t , the transverse displacement of the micro element is expressed by $x(z, t)$. The external loads on the element are in two forms: the distributed external force on unit length of the riser expressed by $f(z, t)$ and the distributed external force moment on unit length expressed by $m(z, t)$.

Morison formula is used to express the internal wave force including horizontal drag force and horizontal inertia force on the riser:

$$f(z, t) = \frac{1}{2}C_D\rho_w Du(z, t)|u(z, t)| + C_M\rho_w \frac{\pi D^2}{4} \frac{du(z, t)}{dt} \quad (1)$$

where C_D is the coefficient of horizontal drag force, C_M is the coefficient of inertia force, D is the outer diameter of riser, ρ_w is the density of seawater, $u(z, t)$ is the horizontal velocity of seawater. Then, ρ_w takes 1025 kg/m^3 , C_D and C_M are 2.0 and 1.2 respectively.

The dynamic equation of the element in the x axial direction can be written as:

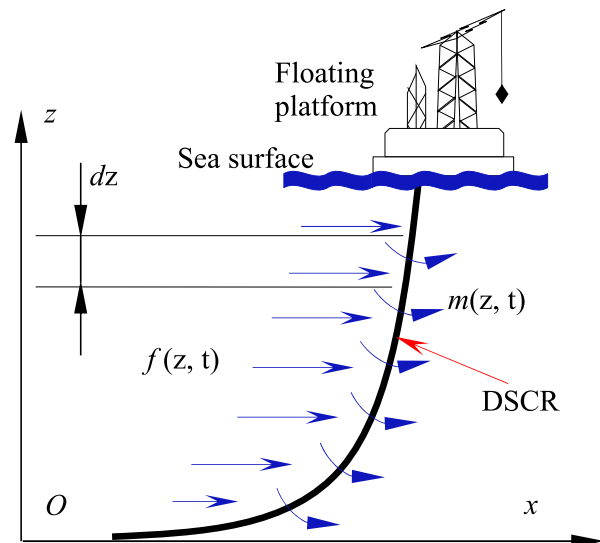


Fig. 1. DSCR system.

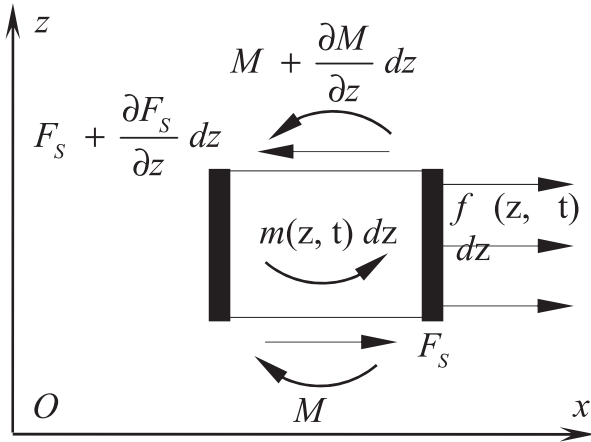


Fig. 2. Forces on the micro element.

$$(\rho_c A_c + \rho_f A_f) dz \frac{\partial^2 x}{\partial t^2} = F_s - \left(F_s + \frac{\partial F_s}{\partial z} dz \right) + f(z, t) dz \quad (2)$$

where F_s is the section shear force, M is the bending moment, ρ_c and ρ_f are densities of the riser and internal fluid, respectively; A_c and A_f are the sectional areas of the riser and internal fluid column, respectively.

Equation (1) is simplified as:

$$(\rho_c A_c + \rho_f A_f) \frac{\partial^2 x}{\partial t^2} = -\frac{\partial F_s}{\partial z} + f(z, t) \quad (3)$$

The moment equilibrium equation of the element is:

$$\begin{aligned} \left(M + \frac{\partial M}{\partial z} dz \right) + m(z, t) dz - M - \frac{dz}{2} f(z, t) dz \\ + \left(F_s + \frac{\partial F_s}{\partial z} dz \right) dz = 0 \end{aligned} \quad (4)$$

Equation (4) contains high-order minor terms $\frac{f(z, t)}{2} (dz)^2$ and $\frac{\partial F_s}{\partial z} (dz)^2$. Omit the quadratic term of dz and simplify it to:

$$F_s = -\frac{\partial M}{\partial z} - m(z, t) \quad (5)$$

Substituting equation (5) into equation (3) gives:

$$\frac{\partial^2 M}{\partial z^2} + \frac{\partial m}{\partial z} = (\rho_c A_c + \rho_f A_f) \frac{\partial^2 x}{\partial t^2} - f(z, t) \quad (6)$$

According to the relationship between the moment and the deflection, one gets:

$$\frac{\partial^2}{\partial z^2} \left(EI \frac{\partial^2 x}{\partial z^2} \right) - (\rho_c A_c + \rho_f A_f) \frac{\partial^2 x}{\partial t^2} = -f(z, t) - \frac{\partial}{\partial z} m(z, t) \quad (7)$$

where E is Young's modulus of the riser; I is moment of inertia of the cross section about the neutral axis.

Since the cross section of the riser is constant, and E and I are constants, equation (7) can be written as:

$$EI \frac{\partial^4 x}{\partial z^4} - (\rho_c A_c + \rho_f A_f) \frac{\partial^2 x}{\partial t^2} = -f(z, t) - \frac{\partial}{\partial z} m(z, t) \quad (8)$$

When $f(z, t) = 0$, and $m(z, t) = 0$, the differential equation of free vibration can be obtained:

$$EI \frac{\partial^4 x}{\partial z^4} - (\rho_c A_c + \rho_f A_f) \frac{\partial^2 x}{\partial t^2} = 0 \quad (9)$$

The solution of equation (8) can be expressed by the product of the function $X(z)$ and the harmonic function of t as:

$$x(z, t) = X(z) (A_1 \cos \omega t + A_2 \sin \omega t) \quad (10)$$

where $X(z)$ is main mode function, ω is natural circle frequency, A_1 and A_2 are the coefficients of the general solution.

Substituting equation (10) into equation (9) gives:

$$\frac{d^4}{dz^4} X(z) = \beta^4 X(z) \quad (11)$$

where $\beta^4 = \frac{\omega^2}{a^2}$, $a^2 = \frac{EI}{\rho_c A_c + \rho_f A_f}$, ω is natural circle frequency.

Then, the general solution of equation (11) is:

$$X(z) = C_1 \sin \beta z + C_2 \cos \beta z + C_3 \sinh \beta z + C_4 \cosh \beta z \quad (12)$$

where C_1 , C_2 , C_3 and C_4 are the coefficients of the general solution.

The traditional steel catenary riser (SCR) is usually directly suspended to a fork support device which is installed on a floating platform. The lower end of the SCR is welded with the submarine pipeline whose boundary conditions can be regarded as a fixed end type. In addition, the authors also designed a hinged riser suspension device to reduce the concentrated force of the suspension end, and the corresponding boundary condition is a hinged restraint. In this paper, the dynamic analysis about both fixed and hinged risers are carried out.

For fixed riser, deflection x and angle $\partial x / \partial z$ are equal to 0:

$$\begin{cases} X(z) = 0 \\ \frac{dX(z)}{dz} = 0 \end{cases} \quad (z=0, \text{ or } z=l) \quad (13)$$

For hinged riser, deflection x and bending moment M are equal to 0:

$$\begin{cases} X(z) = 0 \\ \frac{d^2 X(z)}{dz^2} = 0 \end{cases} \quad (z=0, \text{ or } z=l) \quad (14)$$

2.2. Orthogonality of main modes

When $\omega = p_i$, it corresponds to a main vibration mode $X_i(z)$, and when $\omega = p_j$, it corresponds to another main vibration mode $X_j(z)$. Substituting two groups of solutions $\{p_i^2, X_i(z)\}$ and $\{p_j^2, X_j(z)\}$ into equation (11) gives:

$$\frac{d^2}{dz^2} \left(EI \frac{d^2 X_i(z)}{dz^2} \right) = p_i^2 (\rho_c A_c + \rho_f A_f) X_i(z) \quad (15a)$$

$$\frac{d^2}{dz^2} \left(EI \frac{d^2 X_j(z)}{dz^2} \right) = p_j^2 (\rho_c A_c + \rho_f A_f) X_j(z) \quad (15b)$$

Multiplying both sides of equation (15a) by $X_j(z)$, and both sides of equation (15b) by $X_i(z)$, one gets the integral:

$$\int_0^l X_j \frac{d^2}{dz^2} \left(EI \frac{d^2 X_i}{dz^2} \right) dz = p_i^2 \int_0^l (\rho_c A_c + \rho_f A_f) X_i X_j dz \quad (16a)$$

$$\int_0^l X_i \frac{d^2}{dz^2} \left(EI \frac{d^2 X_j}{dz^2} \right) dz = p_j^2 \int_0^l (\rho_c A_c + \rho_f A_f) X_i X_j dz \quad (16b)$$

Simplify equations (16a) and (16b) by using the partial integral method, one can get:

$$\int_0^l \left(EI \frac{d^2 X_i}{dz^2} \frac{d^2 X_j}{dz^2} \right) dz = p_i^2 \int_0^l (\rho_c A_c + \rho_f A_f) X_i X_j dz \quad (17a)$$

$$\int_0^l \left(EI \frac{d^2 X_i}{dz^2} \frac{d^2 X_j}{dz^2} \right) dz = p_j^2 \int_0^l (\rho_c A_c + \rho_f A_f) X_i X_j dz \quad (17b)$$

Equation (17a) minus Equation (17b), which gives:

$$(p_i^2 - p_j^2) \int_0^l (\rho_c A_c + \rho_f A_f) X_i X_j dz = 0 \quad (18)$$

If $i \neq j$, there must be $p_i^2 \neq p_j^2$, and there will always be:

$$\int_0^l (\rho_c A_c + \rho_f A_f) X_i X_j dz = 0 \quad (i \neq j) \quad (19)$$

Equation (19) shows that the main vibration mode of the riser is orthogonal to the mass. Substituting equation (19) into equation (17) and equation (15) gives:

$$\int_0^l EI \frac{d^2 X_i}{dz^2} \frac{d^2 X_j}{dz^2} dz = 0 \quad (i \neq j) \quad (20)$$

$$\int_0^l X_j \frac{d^2}{dz^2} \left(EI \frac{d^2 X_i}{dz^2} \right) dz = 0 \quad (i \neq j) \quad (21)$$

Therefore, the main vibration mode of the riser is also orthogonal to the stiffness. When $i = j$, equation (18) always holds, then:

$$\int_0^l (\rho_c A_c + \rho_f A_f) X_i^2 dz = M_{pj} \quad (22)$$

$$\int_0^l X_j \frac{d^2}{dz^2} \left(EI \frac{d^2 X_j}{dz^2} \right) dz = \int_0^l EI \left(\frac{dX_j}{dz} \right)^2 dz = K_{pj} \quad (23)$$

where M_{pj} and K_{pj} are the j th order principal mass and principal stiffness, respectively. And the relationship between them by equation (17) is:

$$p_j^2 = \frac{K_{pj}}{M_{pj}} \quad (24)$$

If the normalization condition of the main mode $X_j(z)$ is:

$$\int_0^l (\rho_c A_c + \rho_f A_f) \tilde{X}_j^2 dz = M_{pj} = 1 \quad (j = 1, 2, 3 \dots) \quad (25)$$

Then, the regular mode function is \tilde{X}_j . And, the j th order principal stiffness K_{pj} is equal to p_j^2 .

2.3. Transverse dynamic response

The general solution of equation (8) can be expressed as:

$$x(z, t) = \sum_{i=1}^{\infty} \tilde{X}_i(z) \eta_i(t) \quad (26)$$

where $\tilde{X}_i(z)$ is regular mode function and $\eta_i(t)$ is regular coordinate. Substituting equation (26) into equation (7) gives:

$$\sum_{i=1}^{\infty} \frac{d^2}{dz^2} \left(EI \frac{d^2 \tilde{X}_i}{dz^2} \right) \eta_i - (\rho_c A_c + \rho_f A_f) \sum_{i=1}^{\infty} \tilde{X}_i \ddot{\eta}_i = -f(z, t) - \frac{\partial}{\partial z} m(z, t) \tag{27}$$

Both sides of equation (27) are multiplied by $\tilde{X}_j(z)$, and the integral about z is obtained. Considering the orthogonality and normalization, it can be simplified as:

$$\ddot{\eta}_i + p_i^2 \eta_i = q_i(t) \tag{28}$$

Equation (28) is the differential equation of transverse motion of the riser expressed by the i th regular coordinate. where $q_i(t)$ is:

$$q_i(t) = \int_0^l \left[-f(z, t) - \frac{\partial}{\partial z} m(z, t) \right] \tilde{X}_i(z) dz \tag{29}$$

Equation (29) is the generalized force of the i th regular coordinate.

Set the initial conditions of the DSCR as:

$$\left. \begin{aligned} x(z, 0) &= f_1(z) \\ \frac{\partial x}{\partial t} \Big|_{t=0} &= f_2(z) \end{aligned} \right\} \tag{30}$$

Substituting equation (26) into equation (30), both sides are multiplied by $(\rho_c A_c + \rho_f A_f) \cdot \tilde{X}_i(z)$ and integrated. According to the orthogonality condition, the response of the riser to the initial condition expressed by the regular coordinate can be obtained as:

$$\left. \begin{aligned} \eta_i(0) &= \int_0^l (\rho_c A_c + \rho_f A_f) f_1(z) \tilde{X}_i(z) dz \\ \dot{\eta}_i(0) &= \int_0^l (\rho_c A_c + \rho_f A_f) f_2(z) \tilde{X}_i(z) dz \end{aligned} \right\} \tag{31}$$

The solution of the i th regular coordinate of equation (28) is:

$$\eta_i(t) = \eta_i(0) \cos p_i t + \frac{\dot{\eta}_i(0)}{p_i} \sin p_i t + \frac{1}{p_i} \int_0^t q_i(\tau) \sin p_i(t - \tau) d\tau \tag{32}$$

where τ is a variable about time.

By substituting the response expressed by the regular coordinates of equation (32) into equation (26), the response of the riser to any excitation under the initial conditions is obtained:

$$x(z, t) = \sum_{i=1}^{\infty} \tilde{X}_i \left[\eta_i(0) \cos p_i t + \frac{\dot{\eta}_i(0)}{p_i} \sin p_i t + \frac{1}{p_i} \int_0^t \tilde{X}_i(z) \int_0^t \left(-f(z, t) - \frac{\partial m(z, t)}{\partial z} \right) \sin p_i(t - \tau) d\tau dz \right] \tag{33}$$

3. Dynamic model induced by both axial loads and transverse loads

3.1. Reconstruction of DSCR model

In general, due to the self-weight of the riser and the influence of internal fluid, the riser is subject to axial tension. The total axial force F_T of the riser includes: axial force caused by self-weight of the riser F_c , axial force caused by internal fluid gravity F_f and axial force caused by fluid flowing F_v (see Fig. 3). Then, the total axial force on the riser is:

$$F_T = F_c + F_f + F_v \tag{34}$$

where F_c and F_f are related to the riser density and fluid density respectively, and the wet weight of them in sea water is q_c and q_f respectively. The axial force caused by internal fluid flow is $(R^2/2)\pi\rho_f(v_f)^2$ [5,16], where R , ρ_f and v_f are the inner diameter of the riser, fluid density and fluid velocity, respectively.

The differential equation of transverse motion of the micro element is:

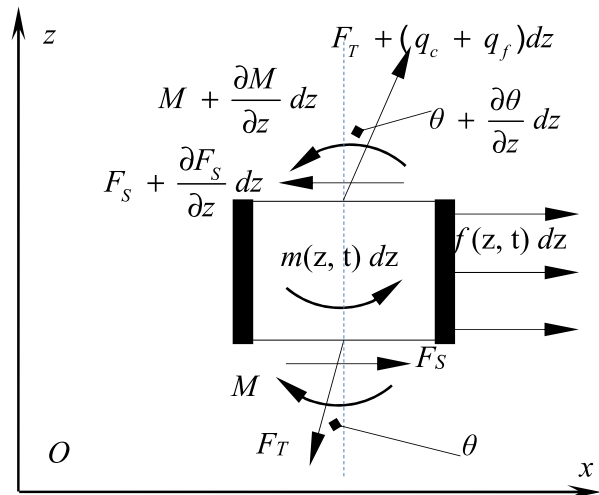


Fig. 3. Element considering longitudinal force.

$$\begin{aligned}
 & [(\rho_c A_c + \rho_f A_f) dz] \frac{\partial^2 x}{\partial t^2} = f(z, t) dz + F_s - \left(F_s + \frac{\partial F_s}{\partial z} dz \right) \\
 & + \left[F_T + (q_c + q_f) dz \right] \cdot \sin \left(\theta + \frac{\partial \theta}{\partial z} dz \right) - F_T \cdot \sin \theta
 \end{aligned}
 \tag{35}$$

where F_s is the section shear force, M is the bending moment, x is the transverse displacement, θ is the angle between the longitudinal load and the axis.

When θ is a smaller angle, one can get $\theta \approx \sin \theta$. Omitting the higher order terms, equation (35) can be simplified as:

$$\frac{\partial F_s}{\partial z} - F_T \frac{\partial \theta}{\partial z} - \theta (q_c + q_f) + (\rho_c A_c + \rho_f A_f) \frac{\partial^2 x}{\partial t^2} = f(z, t)
 \tag{36}$$

Substituting $\theta = \frac{\partial x}{\partial z}$, $F_s = \frac{\partial M}{\partial z}$ and $M = EI \frac{\partial^2 x}{\partial z^2}$ into equation (36) gives:

$$\begin{aligned}
 & \frac{\partial^2}{\partial z^2} \left(EI \frac{\partial^2 x}{\partial z^2} \right) - F_T \frac{\partial^2 x}{\partial z^2} - (q_c + q_f) \frac{\partial x}{\partial z} + \\
 & (\rho_c A_c + \rho_f A_f) \frac{\partial^2 x}{\partial t^2} = f(z, t)
 \end{aligned}
 \tag{37}$$

For free vibration, equation (37) can be written as:

$$\begin{aligned}
 & \frac{\partial^2}{\partial z^2} \left(EI \frac{\partial^2 x}{\partial z^2} \right) - F_T \frac{\partial^2 x}{\partial z^2} - (q_c + q_f) \frac{\partial x}{\partial z} + \\
 & (\rho_c A_c + \rho_f A_f) \frac{\partial^2 x}{\partial t^2} = 0
 \end{aligned}
 \tag{38}$$

The solution of equation (38) is:

$$x(z, t) = X(z) (B_1 \cos pt + B_2 \sin pt)
 \tag{39}$$

where B_1 and B_2 are the coefficients of the general solution.

Substituting equation (39) into equation (38) gives:

$$\frac{d^2}{dz^2} \left(EI \frac{d^2 X}{dz^2} \right) - F_T \frac{d^2 X}{dz^2} - (q_c + q_f) \frac{dX}{dz} - p^2 (\rho_c A_c + \rho_f A_f) X = 0
 \tag{40}$$

where EI is constant because the riser is made of uniform material with constant cross-sectional area. Let $\alpha = \frac{F_T}{EI}$, $\eta = \frac{q_c + q_f}{EI}$, $\beta = p^2 \frac{\rho_c A_c + \rho_f A_f}{EI}$, and then equation (40) can be written as:

$$\frac{d^4 X}{dz^4} - \alpha \frac{d^2 X}{dz^2} - \eta \frac{dX}{dz} - \beta X = 0
 \tag{41}$$

Let the solution of equation (41) be:

$$X(z) = A \cos \gamma z + B \sin \gamma z + C \cosh \lambda z + D \sinh \lambda z
 \tag{42}$$

where λ and γ are circular frequency, and A, B, C, D are the coefficients of the general solution.

Substituting equation (42) into equation (41) gives:

$$\begin{aligned}
 & \gamma^4 A \cos \gamma z + \gamma^4 B \sin \gamma z + \lambda^4 C \cosh \lambda z + \lambda^4 D \sinh \lambda z \\
 & - \alpha (-\gamma^2 A \cos \gamma z - \gamma^2 B \sin \gamma z + \lambda^2 C \cosh \lambda z + \lambda^2 D \sinh \lambda z) \\
 & - \eta (-\gamma A \sin \gamma z + \gamma B \cos \gamma z + \lambda C \sinh \lambda z + \lambda D \cosh \lambda z) \\
 & - \beta (A \cos \gamma z + B \sin \gamma z + C \cosh \lambda z + D \sinh \lambda z) = 0
 \end{aligned}
 \tag{43}$$

When $z = 0$, equation (43) is always true, and then:

$$(\gamma^4 + \alpha \gamma^2 - \beta) A - \eta \gamma B + (\lambda^4 - \alpha \lambda^2 - \beta) C - \eta \lambda D = 0
 \tag{44}$$

3.2. Upper end fixed & lower end fixed (fixed–fixed)

When the upper and lower ends of the riser are both fixed, the transverse displacement and rotation angle of the upper and lower ends of the riser are 0.

Then, the equation of boundary control at the lower end is:

$$\begin{cases} X(z)|_{z=0} = 0 \\ \frac{dX(z)}{dz}|_{z=0} = 0 \end{cases}
 \tag{45a}$$

The equation of boundary control at the upper end is:

$$\begin{cases} X(z)|_{z=l} = 0 \\ \frac{dX(z)}{dz}|_{z=l} = 0 \end{cases}
 \tag{45b}$$

Substituting boundary control equations (45a) and (45b) into equation (41) gives:

$$\begin{cases} A + C = 0 \\ \gamma B + \lambda D = 0 \\ A \cos \gamma l + B \sin \gamma l + C \cosh \lambda l + D \sinh \lambda l = 0 \\ -A \gamma \sin \gamma l + B \gamma \cos \gamma l + C \lambda \sinh \lambda l + D \lambda \cosh \lambda l = 0 \end{cases}
 \tag{46}$$

Equation (46) can be simplified as:

$$\begin{cases} \gamma B + \lambda D = 0 \\ A(\cos \gamma l - \cosh \lambda l) + B \sin \gamma l + D \sinh \lambda l = 0 \\ -A(\gamma \sin \gamma l + \lambda \sinh \lambda l) + B \gamma \cos \gamma l + D \lambda \cosh \lambda l = 0 \end{cases}
 \tag{47}$$

Since equation (47) has solutions, the value of its coefficient determinant is 0, and then, the frequency equation is:

$$(\lambda^2 - \gamma^2) \sinh \lambda l \sin \gamma l - 2\lambda\gamma \cosh \lambda l \cos \gamma l + 2\lambda\gamma = 0 \tag{48}$$

The solution of equation (48) can be expressed by the intersection of two curves:

$$\begin{cases} f_{11}(\lambda, \gamma) = \lambda^2 \sinh \lambda l \sin \gamma l - \lambda\gamma \cosh \lambda l \cos \gamma l + \lambda\gamma \\ f_{12}(\lambda, \gamma) = \gamma^2 \sinh \lambda l \sin \gamma l + \lambda\gamma \cosh \lambda l \cos \gamma l - \lambda\gamma \end{cases} \tag{49}$$

3.3. Lower end fixed & upper end hinged (hinged-fixed)

When the lower end of the riser is fixed and the upper end is hinged, the transverse displacement and rotation angle of the lower end are 0, and the displacement and bending moment of the upper end are 0.

Then, the equation of boundary control at the lower end is:

$$\begin{cases} X(z)|_{z=0} = 0 \\ \frac{dX(z)}{dz}|_{z=0} = 0 \end{cases} \tag{50a}$$

The equation of boundary control at the upper end is:

$$\begin{cases} X(z)|_{z=l} = 0 \\ \frac{d^2X(z)}{dz^2}|_{z=l} = 0 \end{cases} \tag{50b}$$

Substituting equations (50a) and (50b) into equation (41) gives:

$$\begin{cases} A + C = 0 \\ \gamma B + \lambda D = 0 \\ A \cos \gamma l + B \sin \gamma l + C \cosh \lambda l + D \sinh \lambda l = 0 \\ -A\gamma^2 \cos \gamma l - B\gamma^2 \sin \gamma l + C\lambda^2 \cosh \lambda l + D\lambda^2 \sinh \lambda l = 0 \end{cases} \tag{51}$$

Equation (51) can be simplified as:

$$\begin{cases} \gamma B + \lambda D = 0 \\ A(\cos \gamma l - \cosh \lambda l) + B \sin \gamma l + D \sinh \lambda l = 0 \\ -A(\gamma^2 \cos \gamma l + \lambda^2 \cosh \lambda l) - B\gamma^2 \sin \gamma l + D\lambda^2 \sinh \lambda l = 0 \end{cases} \tag{52}$$

Since the coefficient determinant value of equation (52) is 0, the frequency equation is:

$$\lambda \cosh \lambda l \sin \gamma l - \gamma \sinh \lambda l \cos \gamma l = 0 \tag{53}$$

Then, the frequency can be calculated by finding the intersection of function $f_{21}(p)$ and $f_{22}(p)$.

$$\begin{cases} f_{21}(\lambda, \gamma) = \lambda \cosh \lambda l \sin \gamma l \\ f_{22}(\lambda, \gamma) = \gamma \sinh \lambda l \cos \gamma l \end{cases} \tag{54}$$

3.4. Lower end hinged & upper end hinged (hinged-hinged)

When both upper and lower ends of the riser are hinged, the transverse displacement and bending moment at the ends are 0.

Then, the equation of boundary control at the lower end is:

$$\begin{cases} X(z)|_{z=0} = 0 \\ \frac{d^2X(z)}{dz^2}|_{z=0} = 0 \end{cases} \tag{55a}$$

The equation of boundary control at the upper end is:

$$\begin{cases} X(z)|_{z=l} = 0 \\ \frac{d^2X(z)}{dz^2}|_{z=l} = 0 \end{cases} \tag{55b}$$

Substituting boundary control equations (55a) and (55b) into equation (41) gives:

$$\begin{cases} A + C = 0 \\ \gamma^2 A + \lambda^2 C = 0 \\ A \cos \gamma l + B \sin \gamma l + C \cosh \lambda l + D \sinh \lambda l = 0 \\ -A\gamma^2 \cos \gamma l - B\gamma^2 \sin \gamma l + C\lambda^2 \cosh \lambda l + D\lambda^2 \sinh \lambda l = 0 \end{cases} \tag{56}$$

Equation (56) is reduced as:

$$\begin{cases} A = C = 0 \\ B \sin \gamma l + D \sinh \lambda l = 0 \\ -B\gamma^2 \sin \gamma l + D\lambda^2 \sinh \lambda l = 0 \end{cases} \tag{57}$$

The coefficient determinant of equation (57) is 0, and then the frequency equation is:

$$(\lambda^2 + \gamma^2) \sinh \lambda l \sin \gamma l = 0 \tag{58}$$

Since λ , γ and $\sinh \lambda l$ are not 0, $\sin \gamma l = 0$, and then the circular frequency is:

$$\omega_i = \left(\frac{i\pi}{l}\right)^2 \sqrt{\frac{EI}{\rho_c A_c + \rho_f A_f} \left(1 + \frac{F_T l^2}{i^2 \pi^2 EI}\right)} \quad (i=1, 2, 3 \dots) \tag{59}$$

4. Numerical calculation and analysis

To analyze the influence of internal fluid and riser self-weight on the natural frequency of the DSCR, both the velocity and density of internal fluid are considered in this paper. Two assumed cases are:

Table 1. Basic parameters.

No.	Parameter Name	Value
1	Length of the riser l	1300 m
2	Young's modulus E	210 GPa
3	Moment of inertia I	$1.7664 \times 10^{-6} \text{ m}^4$
4	Density of natural gas ρ_{fG}	0.7174 kg/m^3
5	Density of oil ρ_{fO}	810 kg/m^3
6	Density of DSCR ρ_c	7850 kg/m^3
7	Cross-sectional area of DSCR A_c	0.0109 m^2
8	cross-sectional area of internal fluid A_f	0.0885 m^2

the riser with a fluid density of 0 kg/m^3 (empty riser), and that with a fluid density of 500 kg/m^3 (For some oil and gas fields, the product may not be a single natural gas or oil, but may be an oil-gas mixture with a density of about 500 kg/m^3). Three cases of boundary conditions including fixed–fixed end (upper end fixed and lower end fixed), hinged–fixed end (upper end hinged and lower end fixed) and hinged–hinged end (upper end hinged and lower end hinged) are set for the comparative analysis of the dynamic characteristics of the riser. Some basic parameters are given in Table 1:

4.1. Natural frequency of DSCR with fixed–fixed end

The first 21 order vibration frequencies of four riser models with/without internal fluid and with/without considering the riser gravity are shown in Fig. 4.

Notes: No F. & No D.W. refers to without internal fluid and without considering self-weight; No F. & D.W. refers to without internal fluid and considering self-weight; F. & No D.W. refers to with internal fluid and without considering self-weight; F. & D.W. refers to with internal fluid and considering self-weight.

The numerical comparison is as follows: The 1st order frequency of No F. & No D.W. model, No F. &

D.W. model, F. & No D.W. model and F. & D.W. model is 0.0831 rad/s , 0.2751 rad/s , 0.1611 rad/s and 0.2197 rad/s , respectively, and the 21st order frequency is 1.6952 rad/s , 6.0038 rad/s , 3.6365 rad/s and 4.7344 rad/s , respectively.

Due to the large self-weight value of 1300 m riser, weight has a great influence on vibration frequency. Taking the 1st order frequency of non-fluid riser as an example, the frequency of considering self-weight is 3.31 times of that without considering self-weight. If there is internal fluid (500 kg/m^3) in the riser, the 1st order frequency considering self-weight is 1.36 times of that without considering self-weight. Then, internal fluids can increase the inertia of the riser and change the movement of the riser by damping effect. And the vibration frequency of the riser is reduced by 20.13% due to the effect of internal fluid when considering the self-weight of the riser.

If the natural gas density is 0.72 kg/m^3 and the oil density is 810 kg/m^3 , the 1st order frequency of the gas riser is 0.1953 rad/s and that of the oil riser is 0.2365 rad/s , and the latter is 20.08% larger than the former (see Fig. 5). It can be seen that the first 21 order natural frequencies all increase with the density increase of the internal fluid (see Fig. 4 and Fig. 5).

When the fluid velocity in the riser is set as 0 m/s , 5 m/s and 10 m/s , the first 21 order natural frequencies of the gas and oil riser is calculated, as shown in Table 2. The 1st order frequency is 0.2365 rad/s , corresponding to that of the gas riser (0.1953 rad/s) when the flow velocity of internal fluid is 5 m/s , and the 1st order frequency is 0.2368 rad/s , corresponding to that of the gas riser (0.1953 rad/s) when the velocity of internal fluid is 10 m/s , but the increase rate of the oil riser is only 0.09% while that of the gas riser do not change. For the higher order frequency such as the 21st order frequency, the corresponding increase rate of oil riser and gas riser are 0.09% and 0.0002% respectively,

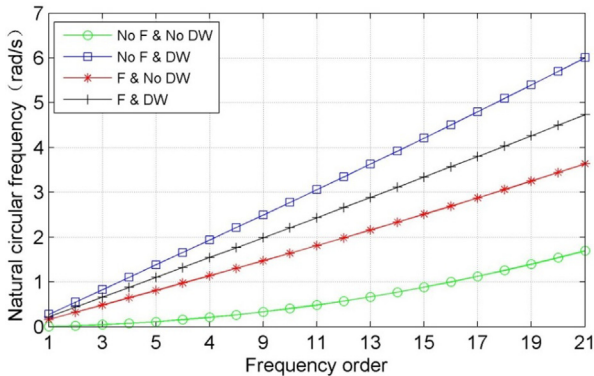


Fig. 4. Frequency comparison of four models (fixed–fixed end).

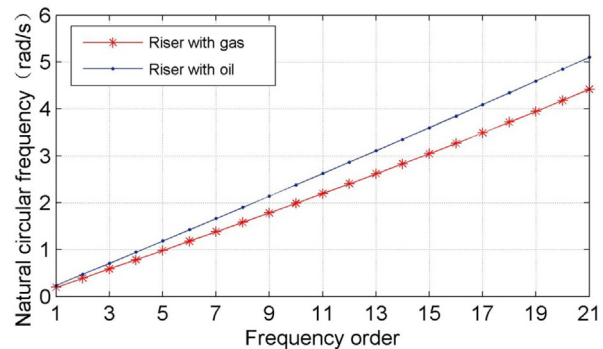


Fig. 5. Frequency comparison of gas riser and oil riser.

indicating that velocity has little effect on the natural frequency, especially when the velocity of internal fluid is very low.

4.2. Natural frequency of DSCR with hinged–fixed end

Similarly, the natural frequencies of four models are obtained (see Fig. 6) when the lower end is fixed and the upper one is hinged.

Notes: No F. & No D.W. refers to without internal fluid and without considering self-weight; No F. & D.W. refers to without internal fluid and considering self-weight; F. & No D.W. refers to with internal fluid and without considering self-weight; F. & D.W. refers to with internal fluid and considering self-weight.

The 1st order frequency of No F. & No D.W. model, No F. & D.W. model, F. & No D.W. model and F. & D.W. model is 0.0857 rad/s, 0.2739 rad/s, 0.1602 rad/s and 0.2135 rad/s, respectively, and the 21st order frequency is 1.6560 rad/s, 5.9778 rad/s, 3.6145 rad/s and 4.5998 rad/s, respectively. The results show that there is a big difference between the models with and without considering self-weight. Due to the increased inertia and damping effects of the internal fluid, the frequency is also slightly reduced when the self-weight is taken into account compared that without fluid.

The first 21 natural frequencies of the non-fluid riser, the gas riser, the contrast group and the oil

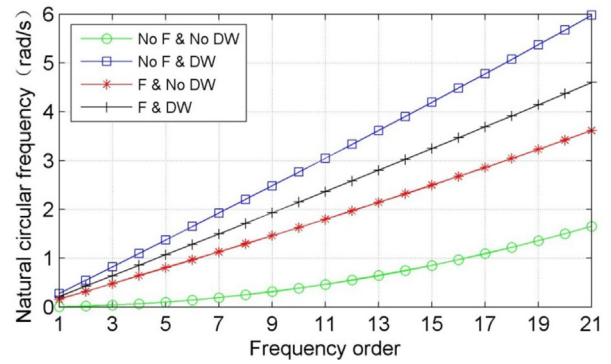


Fig. 6. Frequency comparison of four models (hinged–fixed end).

riser are shown in Table 3. When the fluid velocity in the riser is 0 m/s, the natural frequency of gas riser is close to that of non-fluid riser as the density of natural gas is close to 0 kg/m³. Despite the change in the boundary conditions of the riser, the natural frequency of the riser keeps increasing with the increase of the internal fluid density. For example, the 1st order frequency of gas riser is 0.1941 rad/s and that of the oil riser is 0.2356 rad/s corresponding to an increase rate of 20.38%, and that of the 21st order of 15.85%.

When the boundary conditions of the riser are fixed at the lower end and hinged at the upper end, the first 21 natural frequencies corresponding to the internal fluid velocities of 0 m/s, 5 m/s and 10 m/s are also calculated, as displayed in Table 4. And the influence of fluid velocity on the natural frequency

Table 2. Effect of velocity on natural frequency (fixed–fixed end).

Order	Frequency of gas riser (rad/s)			Frequency of oil riser (rad/s)		
	<i>v</i> = 0 m/s	<i>v</i> = 5 m/s	<i>v</i> = 10 m/s	<i>v</i> = 0 m/s	<i>v</i> = 5 m/s	<i>v</i> = 10 m/s
1	0.1953	0.1953	0.1953	0.2365	0.2365	0.2368
2	0.3908	0.3908	0.3908	0.4731	0.4732	0.4737
3	0.5868	0.5868	0.5868	0.7099	0.7101	0.7108
4	0.7834	0.7834	0.7834	0.9469	0.9472	0.9481
5	0.9809	0.9809	0.9809	1.1843	1.1847	1.1858
6	1.1794	1.1794	1.1794	1.4222	1.4226	1.4241
7	1.3792	1.3792	1.3792	1.6606	1.6611	1.6627
8	1.5804	1.5804	1.5804	1.8996	1.9002	1.9021
9	1.7833	1.7833	1.7833	2.1394	2.1401	2.1421
10	1.9881	1.9881	1.9881	2.3799	2.3806	2.3829
11	2.1949	2.1949	2.1949	2.6213	2.6221	2.6246
12	2.4041	2.4040	2.4040	2.8637	2.8646	2.8673
13	2.6155	2.6155	2.6155	3.1072	3.1081	3.1110
14	2.8296	2.8296	2.8296	3.3518	3.3528	3.3559
15	3.0465	3.0465	3.0465	3.5976	3.5987	3.6021
16	3.2664	3.2664	3.2664	3.8448	3.8460	3.8495
17	3.4895	3.4895	3.4895	4.0934	4.0946	4.0984
18	3.7158	3.7158	3.7159	4.3434	4.3447	4.3487
19	3.9457	3.9457	3.9457	4.5950	4.5964	4.6006
20	4.1791	4.1791	4.1791	4.8482	4.8497	4.8541
21	4.4164	4.4164	4.4164	5.1032	5.1047	5.1093

Table 3. Riser frequency of different density fluid ($v = 0$ m/s).

Order	Natural frequency(rad/s)			
	Non-fluid riser	Gas riser	Contrast group	Oil riser
1	0.1940	0.1941	0.2243	0.2356
2	0.3883	0.3885	0.4487	0.4714
3	0.5830	0.5833	0.6734	0.7073
4	0.7784	0.7787	0.8984	0.9435
5	0.9746	0.9749	1.1239	1.1801
6	1.1718	1.1722	1.3501	1.4171
7	1.3703	1.3708	1.5768	1.6546
8	1.5702	1.5708	1.8045	1.8928
9	1.7718	1.7724	2.0331	2.1317
10	1.9753	1.9759	2.2628	2.3713
11	2.1808	2.1815	2.4936	2.6119
12	2.3885	2.3893	2.7257	2.8534
13	2.5986	2.5995	2.9593	3.0960
14	2.8114	2.8123	3.1943	3.3397
15	3.0269	3.0279	3.4310	3.5847
16	3.2454	3.2464	3.6695	3.8309
17	3.4671	3.4681	3.9097	4.0786
18	3.6920	3.6930	4.1520	4.3277
19	3.9204	3.9215	4.3963	4.5784
20	4.1524	4.1535	4.6427	4.8307
21	4.3881	4.3893	4.8914	5.0848

of this kind of boundary condition is also found very small. It can be seen from Table 4 that all the increase rate is nearly 0% when the flowing velocity of the gas increases from 0 m/s to 5 m/s and from 5 m/s to 10 m/s. But for the oil riser, the maximum increase rate is 0.0318% which is corresponding to the 1st order frequency when the flowing velocity of the oil increases from 0 m/s to 5 m/s, and the maximum

increase rate is 0.0950% when the flowing velocity of the oil increases from 0 m/s to 5 m/s.

4.3. Natural frequency of DSCR with hinged–hinged end

The natural frequencies of four models are also calculated when the upper and lower end of the riser are both hinged (see Fig. 7).

The 1st order frequency of No F. & No D.W. model is 0.0836 rad/s and the 21st order frequency is 1.6173 rad/s; the 1st order frequency of No F. & D.W. model is 0.2727 rad/s and the 21st order frequency is 5.9520 rad/s; the 1st order frequency of F. & No D.W. model is 0.1592 rad/s and the 21st order frequency is 3.5928 rad/s; the 1st frequency of F. & D.W. model is

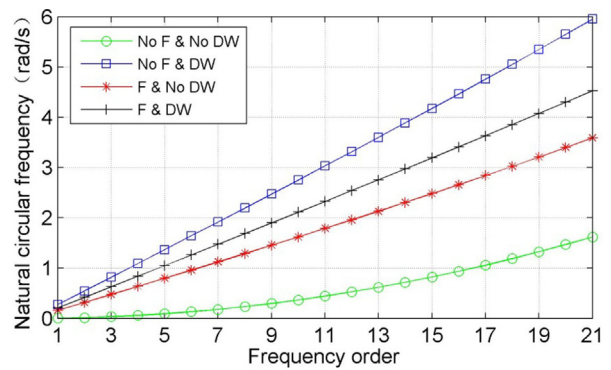


Fig. 7. Frequency comparison of four models (hinged–hinged end).

Table 4. Effect of velocity on natural frequency (hinged–fixed end).

Order	Frequency of gas riser (rad/s)			Frequency of oil riser (rad/s)		
	$v = 0$ m/s	$v = 5$ m/s	10 m/s	$v = 0$ m/s	$v = 5$ m/s	$v = 10$ m/s
1	0.1941	0.1941	0.1941	0.2356	0.2357	0.2359
2	0.3885	0.3885	0.3885	0.4714	0.4715	0.4720
3	0.5833	0.5833	0.5833	0.7073	0.7075	0.7082
4	0.7787	0.7787	0.7787	0.9435	0.9438	0.9447
5	0.9749	0.9749	0.9749	1.1801	1.1804	1.1816
6	1.1722	1.1722	1.1722	1.4171	1.4175	1.4189
7	1.3708	1.3708	1.3708	1.6546	1.6551	1.6567
8	1.5708	1.5708	1.5708	1.8928	1.8934	1.8952
9	1.7724	1.7724	1.7724	2.1317	2.1323	2.1343
10	1.9759	1.9759	1.9759	2.3713	2.3721	2.3743
11	2.1815	2.1815	2.1815	2.6119	2.6127	2.6152
12	2.3893	2.3893	2.3893	2.8534	2.8543	2.8570
13	2.5995	2.5995	2.5995	3.0960	3.0970	3.0998
14	2.8123	2.8123	2.8123	3.3397	3.3408	3.3439
15	3.0279	3.0279	3.0279	3.5847	3.5858	3.5891
16	3.2464	3.2464	3.2464	3.8309	3.8321	3.8357
17	3.4681	3.4681	3.4681	4.0786	4.0798	4.0836
18	3.6930	3.6930	3.6930	4.3277	4.3290	4.3330
19	3.9215	3.9215	3.9215	4.5784	4.5798	4.5840
20	4.1535	4.1535	4.1535	4.8307	4.8322	4.8366
21	4.3893	4.3893	4.3893	5.0848	5.0863	5.0909

Table 5. Riser frequency of different density fluid ($v = 0$ m/s).

Order	Natural frequency(rad/s)			
	Non-fluid riser	Gas riser	Contrast group	Oil riser
1	0.1929	0.1929	0.2233	0.2348
2	0.3860	0.3861	0.4468	0.4697
3	0.5795	0.5797	0.6705	0.7048
4	0.7737	0.7740	0.8946	0.9401
5	0.9687	0.9690	1.1191	1.1758
6	1.1647	1.1651	1.3443	1.4120
7	1.3620	1.3625	1.5701	1.6487
8	1.5607	1.5612	1.7968	1.8860
9	1.7611	1.7617	2.0244	2.1240
10	1.9633	1.9639	2.2531	2.3628
11	2.1675	2.1682	2.4830	2.6025
12	2.3739	2.3747	2.7141	2.8432
13	2.5828	2.5836	2.9467	3.0849
14	2.7942	2.7951	3.1807	3.3277
15	3.0085	3.0094	3.4164	3.5718
16	3.2256	3.2266	3.6538	3.8172
17	3.4459	3.4469	3.8931	4.0639
18	3.6694	3.6705	4.1342	4.3122
19	3.8964	3.8975	4.3775	4.5619
20	4.1270	4.1281	4.6228	4.8133
21	4.3613	4.3624	4.8705	5.0664

0.2101 r rad/s and the 21st order frequency is 4.5250 rad/s. Similarly, when considering the self-weight, the natural frequency decreases slightly with the increase of inertia and damping effect of internal fluid. Therefore, there are great differences between the results with and without considering the self-weight of the model.

Notes: No F. & No D.W. refers to without internal fluid and without considering self-weight; No F. & D.W. refers to without internal fluid and considering self-weight; F. & No D.W. refers to with internal fluid and without considering self-weight; F. & D.W. refers to with internal fluid and considering self-weight.

For the hinged–hinged model, the influence of internal fluid on the natural frequency of the riser is illustrated in Table 5. Taking the 1st order frequency as an example, the increase rate of gas riser, contrast

group and oil riser are 0.0363%, 15.7851% and 21.7272%, respectively, compared with the non-fluid riser. But the corresponding increase rate of the 21st order frequency are 0.0262%, 11.6744% and 16.1681%, respectively. Then, the natural frequency of the riser increases with the increase of the internal fluid density but the amplitude increase of higher order natural frequencies is slightly smaller than that of lower order natural frequencies. Therefore, internal fluid density has a significant effect on the lower order natural frequency.

4.4. Comparison and discussion

To optimize the dynamic characteristics, three kinds of riser ends including hinged–hinged end, hinged-fixed end and fixed–fixed end are studied for the DSCR.

The natural frequencies of each order increase when the boundary condition of the gas riser changes from hinged–hinged end to hinged-fixed end, and the increase amplitude increases obviously with the increase of the order, in which the first order frequency increases by 0.0012 rad/s, while the 21st order frequency increases by 0.0268 rad/s, and the increase amplitude of the larger order in the adjacent order is larger than that of the smaller order (see Fig. 8).

When the boundary condition of the oil riser is changed from hinged–hinged end to hinged-fixed end, the natural frequency of each order increases and the increase rate becomes larger with the increase of order. The 1st order frequency increases by 0.0008 rad/s while the 21st order frequency increases by 0.0183 rad/s. Similarly, the increase value of larger order in the adjacent order is larger than that of smaller order (see Fig. 9).

When the boundary condition is changed from hinged-fixed end to fixed–fixed end, all the natural frequencies of the gas riser increase, in which the 1st order frequency increases by 0.0012 rad/s and the

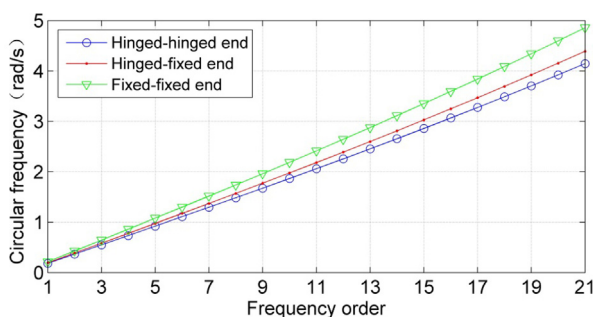


Fig. 8. Relationship between natural frequency and boundary conditions (gas riser).

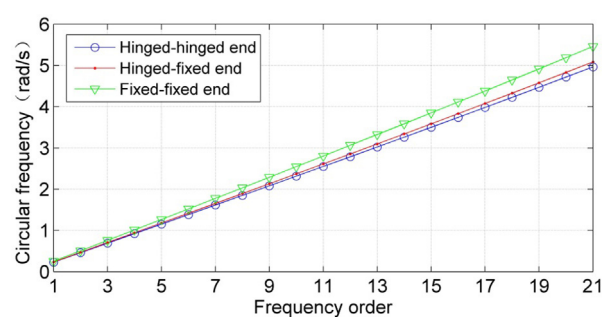


Fig. 9. Relationship between natural frequency and boundary conditions (oil riser).

21st order frequency increases by 0.0271 rad/s. And when the boundary condition is changed from hinged-fixed end to fixed-fixed end, the natural frequencies of oil riser also increase, in which the natural frequency of the 1st order increases by 0.0008 rad/s while the 21st order increases by 0.0175 rad/s. Then, the natural frequency of each order of the gas riser increases gradually when the boundary condition changes from hinged-hinged end to fixed-hinged end and then to fixed-fixed end, and the frequency of oil riser has a similar change trend to that of gas riser.

It can be seen from the figure that under the same boundary conditions, the natural frequency of each order of oil riser is smaller than that of gas riser. This is attributed to the fact that the greater the main mass, the greater the inertia of the riser, the smaller the change in natural frequency.

For non-fluid riser, without considering the axial force caused by self-weight, the 1st order frequency is reduced by 7.03% when the boundary condition changes from fixed-fixed end to hinged-fixed end, while by 13.50% when the boundary condition changes from hinged-fixed end to hinged-hinged end. The corresponding frequency of gas riser decreases by 6.54% and 12.70%, respectively, slightly lower than that of non-fluid riser. Further calculation shows that the natural frequency decreases with the decrease in the number of fixed end. Considering the influence of gravity of the DSCR, the corresponding natural frequency decreases by 0.612% when the boundary condition changes from fixed-fixed end to fixed-hinged end, while by 1.21% when the boundary condition changes from fixed-fixed end to hinged-hinged end.

In addition, the corresponding reduction of the gas riser is about the same as that of non-fluid riser because the density of natural gas is very small and the riser gravity is much larger than that of internal gas. However, that of oil riser decreases by 0.360% and 0.718%, respectively when the boundary

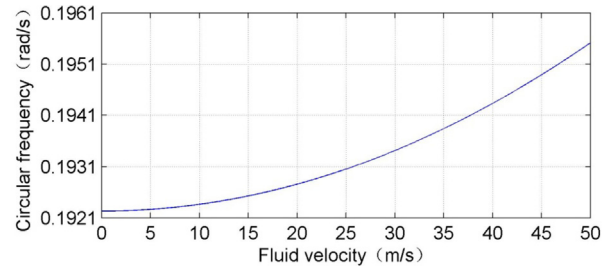


Fig. 11. Relationship between the 1st order frequency and flow velocity (gas riser).

condition are changed. Therefore, the density has little effect on the natural frequency of the riser.

4.5. Change rule of natural frequency due to internal flow (hinged-hinged end)

To study the change trend of natural frequency caused by internal fluid density, the fluid density is set to change within 0–1000 kg/m³. The relationship between the 1st order natural frequency and the density of internal fluid is that the frequency increases with the increase of fluid density, but the increase rate decreases gradually (see Fig. 10). Then, high density fluid slows down the increase rate of riser frequency.

The effect of velocity on natural frequency of gas and oil risers is studied by comparing the two kinds of risers, and the velocity is set to 0 m/s ~50 m/s (see Fig. 11 and Fig. 12). The change trend of gas riser and oil riser are similar to each other.

For the gas riser, when the flow velocity changes from 0 m/s to 5 m/s, the 1st order natural frequency increases by 0.0002 rad/s with an increase rate of 0.104%; when the flow velocity changes from 0 m/s to 30 m/s, the 1st order natural frequency increases by 0.0012 rad/s with an increase rate of 0.625%. It can be seen that as the fluid velocity increases from small to large, the natural frequency increases at an increasing rate. Then, the velocity change of the

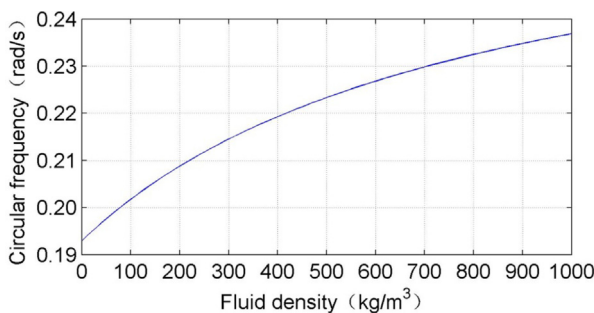


Fig. 10. Relationship between the 1st order natural frequency and the fluid density.

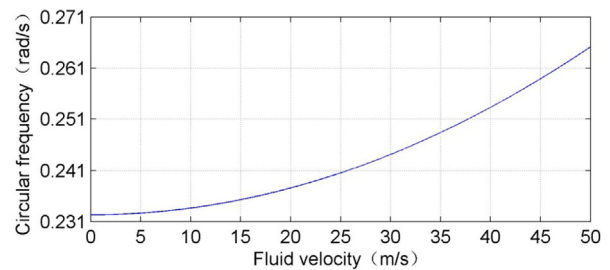


Fig. 12. Relationship between the 1st order frequency and flow velocity (oil riser).

internal fluid at low speed effect the natural frequency of the riser less than that at high speed.

For the oil riser, the 1st order natural frequency increases by 0.0013 rad/s with an increase rate of 0.54% when the internal flow velocity changes from 0 m/s to 5 m/s, and the 1st order natural frequency increases by 0.0121 rad/s with an increase rate of 5.19% when the internal flow velocity changes from 0 m/s to 30 m/s. Similarly, variations in high flow velocity significantly alter the riser frequency.

5. Conclusion

The effects of internal fluid density and velocity on the natural frequency were compared and analyzed by constructing a dynamic model of DSCR. In addition, the differences of natural frequencies of the DSCR with different boundary conditions were studied and analyzed. The following conclusions can be obtained:

- (1) The increase rate of the natural frequency increases gradually with the increase of internal fluid velocity, and the effect of low-speed variation of internal fluid on the natural frequency is smaller than that of high-speed variation. The increase rate of the 1st order natural frequency of gas riser is 0.625%, while that of the 1st order natural frequency of oil riser is 5.19% when the flow rate changes from 0 m/s to 30 m/s. And the frequency of oil riser changed by high-speed fluid is more significant than that of gas riser.
- (2) Without considering the axial force caused by the self-weight of the riser, the 1st order frequency of gas riser decreases by 6.54% when the boundary condition changes from fixed–fixed end to hinged–fixed end, while by 12.70% when the boundary condition changes from hinged–fixed end to hinged–hinged end, but the corresponding reduction of oil riser is less than 1% in both cases. The change of the natural frequency decreases with the increase of the density for the same number of fixed end.
- (3) Considering the effect of the whole self-weight, the 1st order natural frequency of gas riser is reduced by 0.612% when the boundary condition changes from fixed–fixed end to fixed–hinged end and by 1.21% when boundary condition changes from fixed–fixed end boundary condition to hinged–hinged end. The corresponding reductions of oil riser are 0.360% and 0.718%, respectively. The effect of fluid density on the natural frequency becomes smaller when considering the axial force caused by self-weight.
- (4) For the fluid with lower transporting density, the influence of boundary conditions on DSCR natural frequency is greater than that of the fluid with higher transporting density. The dynamic characteristics can be optimized and resonance can be avoided by changing the boundary of the riser and the parameters of internal fluid in practical engineering.

Acknowledgements

Authors gratefully acknowledge the support provided by the Natural Science Foundation of Hunan Province (No: 2019JJ50684; 2020JJ4646), Scientific Research Foundation of Hunan Provincial Education Department (No: 21A0538; 19A046; 21B0766), National Natural Science Foundation of China (NO. 12002067), Special program for scientific research and education of Changsha University in 2021. We deeply appreciate the reviewers' insightful comments and suggestions, which helped a lot in improving the present paper.

References

- [1] Chatjigeorgiou IK. Hydroelastic response of marine risers subjected to internal slug-flow. *Appl Ocean Res* 2017;62: 1–17.
- [2] Chen ZS, Kim WJ, Xiong CB. Effect of upward internal flow on dynamics of riser model subject to shear current. *China Ocean Eng* 2012;26(1):95–108.
- [3] Connaire A, O'Brien P, Harte A, O'Connor A. Advancements in subsea riser analysis using quasi-rotations and the Newton–Raphson method. *Int J Non Lin Mech* 2015;70: 47–62.
- [4] Domingo J, Pérez-Rojas L, Díaz-Ojeda HR. Numerical investigation of vortex-induced vibration of a vertical riser in uniform flow at high Reynolds numbers. *J Mar Sci Technol* 2020;28(1):25–40.
- [5] Guo L, Li G, Liu Y, Zhang G, Wu Z. Overall performance optimization of a spiral pipe type heater by fluid-structure interaction modeling and partitioning screening method. *Case Stud Therm Eng* 2018;11:89–97.
- [6] Hong KS, Shah UH. Vortex-induced vibrations and control of marine risers: a review. *Ocean Eng* 2018;152:300–15.
- [7] Khan RA, Ahmad S. Nonlinear dynamic and bilinear fatigue reliability analyses of marine risers in deep offshore fields. *Ships Offshore Struct* 2018;13(1):10–9.
- [8] Liu Z, Guo H. Sensitivity analysis of steep wave riser with internal flow. *J Mar Sci Technol* 2018;26(4):541–51.
- [9] Meng D, Chen L. Nonlinear free vibrations and vortex-induced vibrations of fluid-conveying steel catenary riser. *Appl Ocean Res* 2012;34:52–67.
- [10] Meng S, Kajiwara H, Zhang W. Internal flow effect on the cross-flow vortex-induced vibration of a cantilevered pipe discharging fluid. *Ocean Eng* 2017;137:120–8.
- [11] Pedersen S, Durdevic P, Yang Z. Challenges in slug modeling and control for offshore oil and gas productions: a review study. *Int J Multiphas Flow* 2017;88:270–84.
- [12] Teixeira DC, Morooka CK. A time domain procedure to predict vortex-induced vibration response of marine risers. *Ocean Eng* 2017;142:419–32.

- [13] Thorsen MJ, Sævik S, Larsen CM. Non-linear time domain analysis of cross-flow vortex-induced vibrations. *Mar Struct* 2017;51:134–51.
- [14] Varas AC, Peters EAJF, Kuipers JAM. CFD-DEM simulations and experimental validation of clustering phenomena and riser hydrodynamics. *Chem Eng Sci* 2017; 169:246–58.
- [15] Wang Q, Duan ML, Li HM, Zhang QY. A singular perturbation method for parametric investigation on J-lay installation of deepwater pipelines. *China Ocean Eng* 2013; 27(6):751–66.
- [16] Xu XX, Gong J. A united model for predicting pressure wave speeds in oil and gas two-phase pipeflows. *J Petrol Sci Eng* 2008;60(3–4):150–60.
- [17] Yu Y, Zhao T, Duan M, Zhou T, Xu J, Su Y, et al. Experimental investigation on the underwater soft yoke mooring system considering sloshing. *Ships Offshore Struct* 2019; 14(3):309–19.